Bulletin of the American Meteorological Society

Co-ordinated Airborne Studies in the Tropics (CAST)

--Manuscript Draft--

Manuscript Number:	BAMS-D-14-00290
Full Title:	Co-ordinated Airborne Studies in the Tropics (CAST)
Article Type:	Article
Corresponding Author:	Neil Harris University of Cambridge Cambridge, UNITED KINGDOM
Corresponding Author's Institution:	University of Cambridge
First Author:	Neil Harris
Order of Authors:	Neil Harris
	Lucy J Carpenter
	James D Lee
	Geraint Vaughan
	Michal T Filus
	Roderick L Jones
	Bin OuYang
	John A Pyle
	Andrew D Robinson
	Steven Andrews
	Alistair C Lewis
	Jamie Minaeian
	Adam Vaughan
	James Dorsey
	Martin W Gallagher
	Michael Le Breton
	Richard Newton
	Carl Percival
	Hugo Ricketts
	Stephane Baugitte
	Graeme Nott
	Axel Wellpott
	Matthew Ashfold
	Johannes Flemming
	Robyn Butler
	Paul Palmer
	Chris Stopford
	Charles Chemel
	Paul Kaye

	Hartmut Boesch
	Neil Humpage
	Andy Vick
	A.R. MacKenzie
	Richard Hyde
	Plamen Angelov
	Alistair Manning
	Elena Meneguz
Manuscript Classifications:	1.088: Maritime Continent; 1.112: Pacific Ocean; 4.172: Convective storms; 4.380: Ozone; 5.008: Aircraft observations
Abstract:	The main field activities of the CAST (Co-ordinated Airborne Studies in the Tropics) campaign took place in the West Pacific in January/February 2014. The field campaign was based in Guam (13.5°N, 144.8°E) using the UK FAAM BAe-146 atmospheric research aircraft and was coordinated with the ATTREX project with the Global Hawk and the CONTRAST campaign with the Gulfstream V aircraft. Together, the three aircraft were able to make detailed measurements of atmospheric structure and composition from the ocean surface to 20 km. These measurements are providing new information about the factors influencing halogen and ozone levels in the tropical West Pacific as well as the importance of trace gas transport in convection for the upper troposphere and stratosphere. The FAAM aircraft made a total of 25 flights between 1°S-14°N and 130°-155°E. It was used to sample at low altitudes (<8 km) with much of the time spent in the marine boundary layer. It measured a range of chemical species and so the region of main inflow into the strong convection was sampled thoroughly. The CAST team also made ground-based measurements of a number of species (including daily ozonesondes) at the Atmospheric Radiation Measurement program site on Manus Island, Papua New Guinea (2.1°S, 147.4°E). This article presents an overview of the CAST project focussing on the design and operation of the West Pacific experiment. It additionally discusses some new developments in CAST, including flights of new instruments on the Global Hawk in February/March 2015.
Author Comments:	This paper is the third of three mentioned originally by Eric Jensen. The first paper is one on ATTREX with Eric Jensen as lead author and the second is one on CONTRAST by Laura Pan. ATTREX, CONTRAST and CAST were three coordinated aircraft campaigns in the West Pacific in early 2014.
Suggested Reviewers:	Bill Randel randel@ucar.edu Expert in TTLS and nvolved in CONTRAS
	Qing Liang Qing.Liang-1@nasa.gov Expert in modelling short-lived bromocarbons and interpreting aircraft measurements
	Isobel Simpson isimpson@uci.edu Expert in interpreting aircraft measurements

Co-ordinated Airborne Studies in the Tropics (CAST)

N. R. P. Harris[1], L. J. Carpenter[2], J. D. Lee[3], G. Vaughan[4], M. T. Filus[1], R. L. Jones[1], B. OuYang[1], J. A. Pyle[1,5], A. D. Robinson[1], S. Andrews[2], A. C. Lewis[2,3], J. Minaeian[2], A. Vaughan[2], J. R. Dorsey[4,6], M. W. Gallagher[6], M. Le Breton[6], R. Newton[6], C. J. Percival[6], H. M. A. Ricketts[4], S. J-B. Baugitte[7], G. J. Nott[7], A. Wellpott[7], M. J. Ashfold[8], J. Flemming[9], R. Butler[10], P. I. Palmer[10], P. H. Kaye[11], C. Stopford[11], C. Chemel[11,12], H. Boesch[13,14], Neil Humpage[13], A. Vick[15], A. R. MacKenzie[16], R. Hyde[17], P. Angelov[17], A. J. Manning[18], E. Meneguz[18].

1. Department of Chemistry, University of Cambridge, Cambridge, UK
2. Department of Chemistry, University of York Cambridge, UK
3. National Centre for Atmospheric Science (NCAS), York, UK
4. National Centre for Atmospheric Science (NCAS), Manchester, UK
5. National Centre for Atmospheric Science (NCAS), Cambridge, UK
6. School of Earth, Atmospheric and Environmental Science, University of Manchester, Manchester, UK
7. Facility for Airborne Atmospheric Measurements, Cranfield, UK
8. School of Biosciences, University of Nottingham Malaysia Campus, Jalan Broga, 43500 Semenyih, Selangor, Malaysia
9. European Centre for Medium-Range Weather Forecasts, Reading, UK
10. School of GeoSciences, University of Edinburgh, Edinburgh, UK
11. Centre for Atmospheric & Instrumentation Research, University of Hertfordshire, Hatfield, UK
12. National Centre for Atmospheric Science (NCAS), University of Hertfordshire, Hatfield, UK
13. Earth Observation Science, Department of Physics and Astronomy, University of Leicester, Leicester, UK
14. National Centre for Earth Observation, University of Leicester, UK
15. UK Astronomy Technology Centre, Edinburgh, UK
16. Birmingham Institute of Forest Research, University of Birmingham, Birmingham, UK
17. Data Science Group, Lancaster University, Lancaster, UK
18. Met Office, Exeter, UK

Corresponding author:
Neil Harris,
Univ. Cambridge Dept. of Chemistry, Lensfield Road, Cambridge, CB2 1EW, UK
Neil.Harris@ozone-sec.ch.cam.ac.uk
Tel.: +44 1223 763816

Abstract

The main field activities of the CAST (Co-ordinated Airborne Studies in the Tropics) campaign took place in the West Pacific in January/February 2014. The field campaign was based in Guam (13.5°N, 144.8°E) using the UK FAAM BAe-146 atmospheric research aircraft and was coordinated with the ATTREX project with the Global Hawk and the CONTRAST campaign with the Gulfstream V aircraft. Together, the three aircraft were able to make detailed measurements of atmospheric structure and composition from the ocean surface to 20 km. These measurements are providing new information about the factors influencing halogen and ozone levels in the tropical West Pacific as well as the importance of trace gas transport in convection for the upper troposphere and stratosphere. The FAAM aircraft made a total of 25 flights between 1°S-14°N and 130°-155°E. It was used to sample at low altitudes (<8 km) with much of the time spent in the marine boundary layer. It measured a range of chemical species and so the region of main inflow into the strong convection was sampled thoroughly. The CAST team also made ground-based measurements of a number of species (including daily ozonesondes) at the Atmospheric Radiation Measurement program site on Manus Island, Papua New Guinea (2.1°S, 147.4°E). This article presents an overview of the CAST project focussing on the design and operation of the West Pacific experiment. It additionally discusses some new developments in CAST, including flights of new instruments on the Global Hawk in February/March 2015.

Capsule: The Co-ordinated Airborne Studies in the Tropics (CAST) project is studying the chemical composition of the atmosphere in the Tropical Warm Pool region to improve understanding of trace gas transport in convection.

Introduction

Co-ordinated Airborne Studies in the Tropics (CAST) is a large multi-institutional project funded by the UK Natural Environment Research Council (NERC) and Science and Technology Facilities Council (STFC). CAST has two overall goals. The first goal is to improve understanding of the tropical atmosphere and how gases move from the surface to the stratosphere. To achieve this, the Facility for Airborne Atmospheric Measurements (FAAM) BAe-146 atmospheric research aircraft was deployed in Guam in January and February 2014 alongside the NASA Global Hawk, a high altitude autonomous aircraft used in the NASA Airborne Tropical Tropopause Experiment (ATTREX) project, and the NSF/NCAR Gulfstream V (GV) in the NSF Convective Transport of Active Species in the Tropics (CONTRAST) project, as described in the companion papers, Jensen et al. (2015) and Pan et al. (2015b). The measurements are being jointly used to diagnose how air is

carried high into the atmosphere. The second CAST goal is to develop the UK capability to use autonomous aircraft for atmospheric research. Here, in addition to learning about deploying the Global Hawk and using the data collected, CAST scientists have produced two new instruments for use on the Global Hawk which flew over the East Pacific in February/March 2015.

The value inherent in having the three aircraft flying together was to be able to measure from the surface up into the stratosphere (see Figure 1 in Pan et al., 2015b). The instrument payloads on the three aircraft made many common measurements which together have combined to provide a comprehensive data set for interpretative studies. However within this larger picture, each aircraft had its own scientific aims and objectives which were appropriate to the specific aircraft capabilities. In the case of the FAAM aircraft, the aims were to (i) investigate halocarbon production in the marine boundary layer, and (ii) characterise the composition of air in the main convective inflow.

The Tropical Tropopause Layer (TTL) is the region of the tropical atmosphere between the main convective outflow at ~12-13 km and the base of the stratosphere at 17-18 km and is a very important region for composition-aerosol-climate interactions (Randel and Jensen, 2013). Its overall structure is intermediate between the troposphere and stratosphere, with a lapse rate smaller than the saturated adiabatic up to the cold point (Fueglistaler et al., 2009). This is caused by the combined effect of slow radiative processes and the infrequent penetration of convective turrets to high altitude. There is a marked longitudinal asymmetry in TTL temperatures, with a minimum in the region 130-180°E at all times of the year. This minimum corresponds to the warm waters of the Tropical Warm Pool (TWP) beneath, and there is an associated similar feature in convection (Gettelman et al., 2002). The TTL is the predominant route for troposphere to stratosphere transport, so that conditions in the TTL set the entry concentrations at the base of the stratosphere for, e.g., stratospheric water vapour and very short-lived halogen species. Knowledge of the input into the TTL is a pre-requisite for correct modelling of TTL (and hence stratospheric) composition and yet many aspects are poorly constrained (Levine et al., 2007; Heyes et al., 2009). The coupling between the various processes are important. For example, improving the treatment of TTL water vapour and cirrus in global climate models requires a better understanding of convective transport and radiative transfer in the TTL, as well as improved model descriptions of the key processes.

We are still unclear about the entry and exit routes for the TTL, including how much material is transported quasi-horizontally into the extratropical lowermost stratosphere (Levine et al, 2008). What is the average residence time in the TTL? What is the nature, and importance for composition, of longitudinal variability within the TTL? How much of the very short-lived (lifetimes < 6 months – VSL) halogen species can pass through the TTL and so affect stratospheric ozone concentrations?

Large discrepancies exist between models and measurements even for long-lived tracers. Some of these are due to transport – sharp horizontal gradients are observed in atmospheric tracers at boundaries between mid-latitude, subtropical and tropical airmasses which are not well represented by models (Wofsy et al., 2011) – and some to limited information on emissions, e.g. N_2O and CH_4 in this region (Ishijima et al., 2010). These issues are likely more important for shorter-lived species, including halogen-containing VSLS with their poorly understood sources, atmospheric transformations and geographic distribution (Carpenter, Reimann et al., 2014).

Knowledge of the distributions of trace gases in the boundary layer and lower troposphere is needed to estimate the flux of these gases into the TTL. The role of the FAAM research aircraft was to fly over the tropical West Pacific and to measure the low level concentrations. These measurements characterise the air masses in the region of the main convective inflow and so are valuable in interpreting the higher altitude measurements of the Global Hawk and the GV made in the same period. They can also be used to improve understanding of marine halocarbon production and to investigate the influence of polluted outflow from south east Asia.

CAST measurements

Measurements were made on two main platforms in the West Pacific. The FAAM BAe-146 research aircraft was based at the A.B. Won Pat International Airport, Guam (13.5°N, 144.8°E). The FAAM aircraft was co-located with the NCAR Gulfstream while the NASA Global Hawk was based at Andersen Air Force Base approximately 30km to the north east. A suite of ground-based instrument systems was based at the Atmospheric Radiation Measurement (ARM) facility at Manus, Papua New Guinea (2.1°S, 147.4°E), in order to characterise the tropospheric composition beyond the range of the FAAM aircraft.

Flight planning

The goal of the CAST FAAM flights was to characterise the inflow to convection in the lower troposphere in the West Pacific. In order to extend the range of the aircraft so that it could reach into the upwelling area nearer the equator, overnight stops were planned at the islands of Palau (Roman Tmetuchl International Airport, Babeldaob island, Republic of Palau; 7.4°N 134.5°E) and Chuuk (Chuuk International Airport, Weno Island, Federated States of Micronesia; 7.5°N, 151.8°E). When conditions allowed, transects were made at 100 feet (with occasional dips down to 50 feet) over the open ocean to give the opportunity to sample air influenced by fresh ocean emissions. Stacked runs with horizontal legs at different altitudes were planned where possible to provide information about the vertical profile of the short-lived species in the lower troposphere. A

large part of the flight planning for the FAAM research aircraft was to ensure a good coverage of the lower troposphere within range from Guam.

Chemical forecast products were also provided by the Monitoring Atmospheric Composition & Climate (MACC) project in support of the field campaigns. MACC assimilates comprehensive global observations of chemical composition into the ECMWF meteorological forecasting system (Flemming et al., 2015). The operational MACC system runs at 80 km horizontal resolution (T255) with 60 vertical levels. During the campaign, forecast plots for the operation domain were provided for a number of chemical species, including the FAAM measurements O_3, CO, CH_4, black carbon, NO, and NO_2. In addition, a number of hypothetical tracers were included to track air originating from different locations, e.g. regional emissions from China or India. A coastal emission tracer was used since $CHBr_3$ and other short-lived halocarbons are preferentially released in coastal regions (Carpenter et al., 2009; Ashfold et al., 2014).

FAAM BAe-146 aircraft

The FAAM BAe-146 has a science payload of up to 4 tonnes designed according to the objectives of a particular campaign. The chemical composition of the tropical atmosphere is the focus of CAST and this dictated the scientific payload. The chemical species and physical parameters measured on the FAAM aircraft, along with the instruments used, are summarised in Table 1. Trace gases with a wide range of atmospheric lifetimes, sources and sinks were measured in order to provide information about the origin and fate of the air masses encountered as well as about the atmospheric timescales involved. In many cases these species were also measured by the Global Hawk and/or the GV aircraft giving good synergy between the three datasets. Understanding the distribution and chemistry of halogen species is a special focus for all three campaigns and this is reflected in the FAAM payload.

Whole air samples (WAS) were collected as described in Andrews et al. (2013). Analysis of WAS canisters was carried out in the aircraft hangar, usually within 72 hours of collection. Two litres of sample air were pre-concentrated using a thermal desorption unit (Markes Unity2 CIA-T) and analysed with gas chromatography, mass spectrometry (GC-MS, Agilent 7890 GC, 5977 Xtr MSD). Halocarbons were quantified using a NOAA calibration gas standard, dimethylsulphide was quantified using a secondary standard prepared and referenced to a primary KRISS standard. The full method is detailed in Andrews et al. (2015).

Measurements of a subset of halocarbons and other volatile organic compounds (VOCs) were made in-flight using a new thermal desorption (TD) GC-MS system. 1 L of sample air, drawn from a window blank inlet, pressurised to 2.5 atm and dried using a multi-core counter-current Nafion drier

was alternately pre-concentrated or analysed from two parallel adsorption traps (Tenax TA) of a two channel TD system (Markes International, model TT 24/7). Analytes were refocussed at the head of the column using liquid CO_2 prior to separation (10 m, 180 micron I.D., 1 micron film, Restek RTX502.2 column; 40 to 150 °C at 40 °C/min) by GC (Agilent 6850) and detection by electron impact MS single ion monitoring (Agilent 5975C), calibrated pre-flight against the WAS gas standard (NOAA, SX-3581). Instrument temporal resolution, and associated sample integration period, was 5 min.

The chemical ionisation mass spectrometer (CIMS) from the Georgia Institute of Technology was configured similarly to previous deployments (Le Breton et al., 2012; 2013). The I^- ionization scheme was used to detect inorganic halogens, carboxylic acids, HCN and other trace species. For CAST, the CIMS made simultaneous measurements of BrO, BrCl, Br_2 and HOBr. The 1 Hz data were averaged to 30 s for analysis. Pre campaign and post flight laboratory calibrations were used relative to in-flight formic acid calibrations to quantify the sensitivities and limits of detection for the inorganic halogens, similar to that used for dinitrogen pentoxide (Le Breton *et al.,* 2014). The sensitivities ranged from 1 to 50 ion counts ppt^{-1} s^{-1} determined by in-flight and post campaign calibrations. The limits of detection for species varied from 0.36 ppt to 37 ppt for 30 s averaged data. (All mixing ratios given in this paper are by volume.) An acid scrubber was used to quantify background signal in the instrument and inlet line.

A broadband cavity enhanced absorption spectrometer (BBCEAS) was adapted to measure IO in the 410-482 nm wavelength region using. No clear absorption feature was observable from spectra by eye with up to 100 s averaging, pointing to very low mixing ratios (<~0.5 ppt) of IO over the sampled area. When using averaged data, a small positive bias (~0.3 ppt) of IO was observed with respect to the zero. These observations appear to support the existence of IO in the remote marine boundary layer at sub-ppt levels, but the limited sensitivity precludes robust identification of spatial gradients.

NO was measured using the well known chemiluminescence technique. NO_2 was quantified using a second channel, with NO_2 being converted to NO using a blue light LED converter centred at 395 nm. The NO_2 mixing ratio is derived from the difference between total NO_x and NO mixing ratios. The instrument is calibrated via addition of 5 sccm of known NO concentration to the ambient sample. The conversion efficiency of the LED converter is measured in each calibration using gas phase titration of the NO to NO_2 on addition of O_3. In flight calibrations were conducted above the boundary layer to ensure stable low levels of NO_x with before and after flight calibrations made using an overflow at the inlet of zero grade air. A more detailed description of a similar system can be found in Lee et al. (2009).

206 O_3 was measured by a UV absorption photometer (Thermo Fisher, model 49C), traceable to the UK
207 National Physical Laboratory primary ozone standard with an uncertainty of 2%, and a precision of
208 1 ppb for 4 s measurements.

209 CO was measured by a vacuum UV fluorescence analyser (Aero Laser GmbH, model AL5002,
210 Gerbig et al., 1999). The instrument was calibrated in-flight every ~45 minutes using a synthetic air
211 working standard (Air Liquide, ~500 ppb), traceable to the NOAA-Earth System Research
212 Laboratory (GMD-CCGG) surveillance standard and the World Meteorological Organisation CO
213 scale X2004. 1Hz CO measurements have a 2% uncertainty and 3 ppb precision.

214 CO_2 and CH_4 were measured by a cavity-enhanced IR absorption spectrometer (Los Gatos Research
215 Inc. Fast Greenhouse Gas Analyser, model RMT-200). The instrument was customised for airborne
216 operation (O'Shea et al, 2013), so CO_2 and CH_4 dry mole fractions can be linearised in-flight using
217 natural air working standards, traceable to the World Meteorological Organisation CO_2 scale X2007
218 and CH_4 scale X2004. The performance of the system is estimated from the 1σ standard deviation
219 of all in-flight 'target' calibration data. The 1Hz measurement precisions are estimated at 0.7 ppm
220 and 2.5 ppb for CO_2 and CH_4. Through the addition of all known uncertainties we estimate a total
221 accuracy of ±1.3 ppb for CH_4 and ±0.2 ppm for CO_2.

222 The Passive Cavity Aerosol Spectrometer Probe 100-X (PCASP), upgraded with the SPP-200
223 electronics package from Droplet Measurement Technologies (DMT), measures aerosol particles
224 with nominal diameters 0.1 to 3 μm. Light from a 0.6328 μm laser is scattered by the particles and a
225 photodetector sums the forward (over solid angles subtended by 35°-120°) and backward (60°-
226 145°) scattered light. The probe is canister-mounted under the wing and was operated at 1 Hz. The
227 instrument was calibrated for particle size before and after the campaign. Uncertainties exist in both
228 the sizing and counting of particles and these are discussed, along with the calibration procedure, in
229 Rosenberg et al. [2012].

230 The DMT Cloud Droplet Probe (CDP; Lance et al., 2010) was flown on the same under-wing pylon
231 as the PCASP. The CDP is an open path instrument that measured the forward scattered light (over
232 solid angles nominally subtended by 1.7°-14°) from the 0.658 μm incident laser beam. Particles are
233 assigned to one of thirty size bins over the nominal size range 3-50 μm. Calibration with certified
234 diameter glass beads was carried out before each flight (Rosenberg et al., 2012). The sample rate of
235 the CDP was the same as for the PCASP, 1 Hz.

236

237 ***Manus***

Observations started at the ARM Climate facility on Manus Island in October 1996 (Mather et al, 1998) and continued until August 2014. These observations provided the basis for many studies of the climate in the West Pacific (e.g., Long et al., 2013 and references therein). In February 2014, a suite of ground-based instruments was deployed as part of CAST to make measurements of ozone (ground and profile), short-lived halocarbons, carbon dioxide, carbon monoxide and methane. The instruments used are now described and are summarised in Table 2.

Ozone profiles were measured using ozonesondes. Air is pumped through a KI solution in a cathode half-cell, with two electrons produced for each ozone molecule; the cell current is directly proportional to the flow of ozone through the cell. Ozonesondes have a typical response time of ~ 1 minute at the tropopause level, with a precision of a few ppb. In the TTL the accuracy of the measurement is dominated by the background current (Newton et al 2015 and references therein). Simultaneous vertical profiles of ozone, temperature, humidity, wind and pressure are measured using a radiosonde.

Ground-level ozone was measured by a Thermo-Electric Corporation TE49C which is a dual-channel ultraviolet photometer measuring ozone through absorption of radiation at 254 nm. The incoming air stream is split between two identical cells, with a scrubber removing ozone from one of the streams. The TE49C provides a measurement every 10 s and has a 20 s response time.

Ground-level trace gas concentrations were measured by a Picarro Cavity Ring-Down Spectrometer G2401 (CRDS) (Crosson, 2008). The sample air inlet was at ~8 m above ground level with a rain cover and a 2 μm particulate filter. Water vapour in the instrument was kept below 1.5 ppm and was controlled by passing the sample flow (~250 mL min^{-1}) through a chiller at ~5 °C and then through a dessicant based nafion drier. CO_2 and CH_4 concentrations were recorded every 5 s, with precisions of ~1 ppb and ~200 ppb respectively. Calibrations were achieved using a target gas (CH_4, 2024 ppb; CO_2, 390 ppm) measured every 2 days for 10 minutes with low / high calibration runs on intermediate days (low/high: CH_4, 1919/2736 ppb; CO_2, 360/495 ppm). The calibration gases are linked to the NOAA/WMO calibration scale.

Surface concentrations of short-lived halocarbons were measured using a μDirac instrument, a gas chromatograph with electron capture detector (GC-ECD) based on that described in Gostlow et al (2010) but with a 10 m separation column. The instrument sampled ambient air from the ~ 8 m high mast, with a 10-20 ml min^{-1} flow dried using a counter flow nafion drier. Calibration runs, using a NOAA-ESRL air cylinder spiked with the target compounds, were conducted regularly (every 3 samples). The calibration volumes ranged from 3 to 50 ml to allow correction for drifts in instrument sensitivity and linearity. Measurement precision is species dependent, typically 2-10 % (±1sd), with accuracy in the range 5-10 % (±1sd).

272

273 **Overview of measurements**

274 The FAAM BAe-146 made a total of 25 science flights with 90 flight hours during the CAST
275 deployment in the West Pacific (Figure 1). Brief summaries of the flights are given in Table 3. The
276 flight tracks are shown in Figure 1, with the altitude represented by the colour of the line. The large
277 majority of the flights were below 5 km altitude, with a significant fraction in the marine boundary
278 layer, with good coverage between 130°E-160°E and 2°S-14°N.

279 The vertical distribution of the science flights can also be seen in Figure 2 which shows O_3 and CO
280 concentrations as a function of altitude and latitude. In general lower O_3 values are found in the
281 marine boundary layer and at lower latitudes, while high values are found at higher altitudes and at
282 higher latitudes. There is no obvious correlation with CO. However when the O_3 and CO data are
283 plotted against each other (Figure 3), a bimodal relationship emerges. Further, the lower ozone
284 values (10-40 ppb) occur when the relative humidity is high (Figure 3, top panel). This finding
285 reinforces that of Pan et al. (2015a) who report this bimodality throughout the altitude range
286 covered by the NCAR GV. They argue that the CONTRAST measurements reveal a bimodal
287 distribution of tropospheric ozone with a background mode of nearly constant (~20 ppb) values
288 throughout the troposphere with a secondary mode of higher ozone in layers with lower relative
289 humidity consistent with advection and mixing from outside the deep tropics. Our measurements
290 also show that high ozone and lower relative humidity often occurs with higher NO and CO
291 concentrations. Preliminary analysis of the high NO measurements indicates that the air masses
292 encountered had previously been in regions close to anthropogenic activities and/or biomass
293 burning. The MACC forecasts also show transport of biomass burning and SE Asian tracers to the
294 West Pacific.

295 The $CHBr_3$ concentrations measured with the Whole Air Sampler and the on-board GC-MS are
296 shown in Figure 4. In general the values are low with even the higher values not far above the
297 background values seen in this region (Brinckmann et al., 2012). The lower amounts of $CHBr_3$ were
298 encountered out of the boundary layer (Figure 4b). The background in Figure 1 shows that the
299 Chlorophyll-a concentrations in the surface waters of the West Pacific were low in this period.
300 Higher Chl-a values are seen in the shallower waters approaching the islands of the Maritime
301 Continent. The lagoon inside Chuuk atoll is relatively shallow (<60 m) and is embedded in much
302 deeper ocean waters. It has a circumference of ~200 km and an area of ~3000 km^2. If halocarbons
303 are emitted preferentially in shallow waters (Carpenter et al., 2009), then it should be discernible as
304 an emission hotspot. The influence of short-lived halocarbon emissions from shallower waters was
305 investigated in the FAAM flights by circling Chuuk atoll at low altitudes. The inset of Figure 4a

306 shows the $CHBr_3$ observed on these flights as well as the instantaneous wind speed observed by the
307 FAAM aircraft. Higher concentrations of $CHBr_3$ (red) are found when air has previously passed
308 over the atoll, indicating that the atoll is a source of $CHBr_3$.

309 $CHBr_3$ was also observed at the ARM facility in Manus (Figure 5). The median value in this period
310 was 0.81 ppt, about half what has been observed at a coastal site in Malaysian Borneo (Robinson et
311 al., 2014) and similar to the values observed on the FAAM aircraft (Figure 4). A strong diurnal
312 cycle is seen in early February in several trace gases measured at Manus with increased nocturnal
313 amounts providing evidence for local night-time sources of CO_2, CH_4, $CHBr_3$ and CH_3I. This
314 diurnal behaviour was seen when the winds were low and a stable boundary layer was able to form.
315 Ozone, by contrast, showed decreases at night in this period from a peak daytime value of 10 ppb to
316 sub 5 ppb levels which are consistent with oxidative uptake to the local vegetation. This is the only
317 time such low values of ozone were seen in CAST. In the absence of local sources, C_2Cl_4 is a good
318 tracer of large scale transport, and its concentrations in this period were generally in the range 1-1.5
319 ppt which are typical of those seen in the clean West Pacific (Ashfold et al., 2015). Manus was
320 mainly influenced by flow from the north in this period

321 A total of 39 ozonesondes were launched from Manus in February 2014, with 34 sondes providing
322 good ozone profiles (Figure 6(a); Newton et al., 2015). These measurements are hardest in the
323 tropics as the ozone concentrations are low, so that any error in estimating the background current is
324 important. Particular attention was therefore paid to measurements of the background current,
325 leading to recommendations for changes to the standard operation procedures used in the sonde
326 preparation. Support for this approach is provided by good agreement in a coordinated ozonesonde /
327 GV flight (see Figure 14 in Pan et al., 2015b). The ozone measurements are shown in Figure 6
328 alongside the corresponding MACC 1 and 4 day forecasts. The forecasts predicted the main
329 characteristics of the observations such as increased ozone at about 400 hPa from 14-16 Feb and the
330 low concentrations near the TTL from 19-23 Feb. The minimum reproducible ozone concentration
331 measured in the TTL was 12 ppb, consistent with the minimum of 13 ppb measured by the GV
332 during CONTRAST (Pan et al., 2015).

333

334 **Linking measurements**

335 In order to have near-real-time information about the air reaching the TTL from the lower
336 troposphere, the trajectory-based approach of Ashfold et al (2012) was adapted to meet the needs of
337 a multi-aircraft campaign. In this, the Numerical Atmospheric-dispersion Modelling Environment
338 (NAME) was run as an adjunct to the Met Office operational forecasting model so that it could
339 access meteorological forecasts on a timescale quick enough to provide useful flight planning

information. The starting grid for the trajectories covered a large area of the West Pacific (Figure 7), with trajectories being released at altitudes between 8 and 18 km. Twelve day backward trajectories were then calculated using a mixture of Met Office analyses and forecasts, so that information was available about the possible influence of lower tropospheric air in the regions which could be sampled by the Global Hawk and the GV. Each day, trajectories were produced for 1, 2, 3 and 5 days in the future. In each 2 km altitude layer, 5,000 particles were released in each 10º x 10º box. During the campaign, these calculations were made for a larger area at higher altitudes to reflect the larger range of the Global Hawk. The horizontal resolution of the Met Office operational model was 25 km in early 2014.

An example is shown in Figure 7 for three altitude ranges (12-14 km, 14-16 km, and 16-18 km). Each point is the end-point of each parcel of air that had crossed below 1 km in the preceding 12 days. For graphical clarity, only a fraction of the trajectories are shown at each level. Thus the stronger the predicted low level influence is shown in total by the higher the percentage in each box (shown by the number), and at a given level by the denser clouds. These maps were routinely checked against flight plans for the Global Hawk and the GV to ensure that a wide range of low level influence was sampled. In general, most flight plans met this criteria due to the proximity of the aircraft to the main convective region. A similar approach using Met Office analysed fields is being used to interpret the measurements of the Global Hawk and GV and to link them back to the lower altitude measurements made by the FAAM aircraft (e.g., Navarro et al., 2015).

New technology developments

As part of the collaboration with ATTREX, three new developments were included in CAST: two instruments for use on the Global Hawk, the Aerosol-Ice-Interface Transition Spectrometer (AIITS) and the GreenHouse gas Observations in the Stratosphere and Troposphere (GHOST); and a software tool, Real-time Atmospheric Science Cluster AnaLysis (RASCAL), designed to assist aircraft scientists by performing real-time data analysis during flights. The two new instruments were flown for a total of 40 hours in one test flight and two science flights in February-March 2015 from the NASA Armstrong Flight Research Center, California. They were part of a payload which also included Hawkeye, the NOAA H_2O and O_3 instruments, the Global Hawk Whole Air Sampler (GWAS), and Microwave Temperature Profiler (MTP) (see Jensen et al, 2015 for more details).

The Aerosol-Ice-Interface Transition Spectrometer (AIITS) was designed to probe different cirrus regimes in the TTL in order to understand fundamental nucleation and sublimation processes influencing the stratospheric water budget and fluxes, as well as the potential impact of biomass burning on cirrus ice crystal activation and growth. It is the next instrument in the Small Ice

Detector (SID) family (Hirst et al., 2001; Kaye et al., 2008). AIITS acquires 2-D forward scattering patterns from particles in the size range from about one to a few hundred micrometres and can measure the depolarisation in backward and forward scattering. The patterns allow quantification of the phase, habit and fine surface features of large aerosol and small ice crystals in the size range 2-100 μm (Cotton et al., 2010; Ulanowski et al., 2014). Unique results were obtained by AIITS during cirrus penetrations at 16.5 km and at temperatures down to -80°C (Figure 8). These revealed a transition to smooth quasi-spherical ice particle regimes in specific regions of TTL layers in response to changing supersaturation regimes. The impact on the radiative scattering properties of cirrus in these regimes is being investigated.

GHOST is a novel grating spectrometer designed for remote sensing of greenhouse gases from aircraft (Humpage et al., 2014). It measures spectrally-resolved shortwave-infrared radiance across four spectral bands from 1.27 μm to 2.3 μm, with a spectral resolution between 0.1 and 0.3 nm. An optical gimbal underneath the aircraft is programmed to pass solar radiation reflected from the ocean surface through a fibre optic bundle into the spectrometer with a single grating and detector for all 4 bands. The bands are chosen to include absorption bands for CO_2 and CH_4 as well as CO, H_2O and O_2. O_2 is used to infer information on the scattering contributions towards the measured light. The third Global Hawk flight of the CAST/ATTREX campaign targeted the overpasses of two greenhouse gas observing satellites during clear sky conditions over the Eastern Pacific (Figure 9); the NASA Orbiting Carbon Observatory (OCO-2) and the JAXA Greenhouse gas Observing SATellite (GOSAT). This Global Hawk flight therefore provides a very useful validation dataset for these satellites, since they both make greenhouse gas measurements using a similar spectral range to GHOST.

As real-time data becomes increasingly available, mission scientists are faced with a potentially overwhelming data torrent from which they are required to find the information on which to base decisions. At present, mission scientists often focus on a subset of the data stream, limiting the depth of the analysis which can be carried out. As part of CAST, a new software framework, RASCAL, has been developed. It interfaces intuitively with mission scientist expert knowledge and provides real-time on-the-fly cluster and anomaly detection (i.e. for real-time diagnosis of structures such as those diagnosed in Figure 3, for example, but tested simultaneously across many chemical 'dimensions'). The data stream can be separated in real-time, without a priori assumptions about parameter relationships, to reveal different data groups and hence isolate specific regions of interest that can be revisited virtually post-flight. In combination with the expert knowledge of the mission scientists, support tools like RASCAL have the potential to be used on many research aircraft, potentially adding significant value to the results achieved in field measurement campaigns.

408

409 **Summary**

410 Based in Guam as part of a joint deployment with the NASA ATTREX Global Hawk and the NSF
411 CONTRAST GV, the FAAM research aircraft deployment in CAST has provided an excellent
412 characterisation of the lower tropospheric atmospheric composition in the Tropical Warm Pool
413 region. The majority of the FAAM aircraft flights were below 5 km altitude, and a significant
414 fraction was in the marine boundary layer with good coverage in 130°E-160°E and 2°S-14°N. A
415 suite of organic and inorganic halogen compounds was measured, with the bromine-containing
416 species particularly well covered.

417 Ground-based measurements were made at the ARM facility on Manus Island, Papua New Guinea
418 during February 2014. These measurements characterise the tropospheric composition just south of
419 the equator in a region inaccessible to the FAAM aircraft in this deployment. The Manus
420 ozonesonde measurements are a valuable resource, providing a good picture of the vertical
421 distribution of ozone in the Tropical Warm Pool region during February with a minimum ozone
422 concentration in the TTL of 12 ppb.

423 These measurements are being interpreted by CAST scientists in conjunction with measurements
424 from ATTREX and CONTRAST using a range of modelling and data analysis approaches. The
425 CAST data are stored at the British Atmospheric Data Centre (http://badc.nerc.ac.uk/), and
426 interested parties are encouraged to use them for their own studies. All users are strongly
427 encouraged to involve the responsible instrument scientists in these studies in order to have insight
428 into the strengths and weaknesses of these data.

429

430 **Acknowledgements**

431 CAST is funded by NERC and STFC, with grant NE/ I030054/1 (lead award), NE/J006262/1,
432 NE/J006238/1, NE/J006181/1, NE/J006211/1, NE/J006061/1, NE/J006157/1, NE/J006203/1,
433 NE/J00619X/1, and NE/J006173/1. N. R. P. Harris was supported by a NERC Advanced Research
434 Fellowship (NE/G014655/1). P. I. Palmer acknowledges his Royal Society Wolfson Research Merit
435 Award. The BAe-146-301 Atmospheric Research Aircraft is flown by Directflight Ltd and managed
436 by the Facility for Airborne Atmospheric Measurements, which is a joint entity of the Natural
437 Environment Research Council and the Met Office. The authors thank the staff at FAAM,
438 Directflight and Avalon Aero who worked so hard toward the success of the aircraft deployment in
439 Guam, especially for their untiring efforts when spending an unforeseen 9 days in Chuuk. We thank
440 the local staff at Chuuk and Palau, as well as the authorities in the Federated States of Micronesia
441 for their help in facilitating our research flights. Special thanks go to the personnel associated with

the ARM facility at Manus, Papua New Guinea without whose help the ground-based measurements would not have been possible. Thanks to the British Atmospheric Data Centre (BADC) for hosting our data and the NCAS Atmospheric Measurement Facility for providing the radiosonde and ground-based ozone equipment. Chlorophyll-a data used in Figure 1 were extracted using the Giovanni online data system, maintained by the NASA GES DISC. We also acknowledge the MODIS mission scientists and associated NASA personnel for the production of this data set. Finally we thank many individual associated with the ATTREX and CONTRAST campaigns for their help in the logistical planning, and we would like to single out Jim Bresch for his excellent and freely provided meteorological advice.

References

Acker, J. G., and G. Leptoukh, 2007: Online Analysis Enhances Use of NASA Earth Science Data. *Eos, Trans.*, **88,** 2, 14-17.

Allen, G., and Coauthors, 2011: South East Pacific atmospheric composition and variability sampled along 20° S during VOCALS-Rex. *Atmos. Chem. Phys.*, **11**, 5237-5262, doi:10.5194/acp-11-5237-2011.

Andrews, S. J., C. E. Jones, and L. J. Carpenter, 2013: Aircraft measurements of very short-lived halocarbons over the tropical Atlantic Ocean. *Geophys. Res. Lett.*, **40**, 1005–1010, doi:10.1002/grl.50141.

Andrews, S.A. and Coauthors, 2015: A comparison of very short-lived halocarbon (VSLS) aircraft measurements in the West Tropical Pacific from CAST, ATTREX and CONTRAST. *Submitted to ACPD*.

Ashfold, M.J., N.R.P. Harris, E.L. Atlas, A.J. Manning and J.A. Pyle, 2014: Transport of short-lived species into the Tropical Tropopause Layer. *Atmos. Chem. Phys.*, **12**, 6309-6322, doi:10.5194/acp-12-6309-2012.

Ashfold, M. J., N. R. P. Harris, A. J. Manning, A. D. Robinson, N. J. Warwick, and J. A. Pyle, 2014: Estimates of tropical bromoform emissions using an inversion method. *Atmos. Chem. Phys.*, **14**, 979–994, doi:10.5194/acp-14-979-2014.

Ashfold, M. J., and Coauthors, 2015: Rapid transport of East Asian pollution to the deep tropics. *Atmos. Chem. Phys.*, **15**, 3565-3573, doi:10.5194/acp-15-3565-2015.

Brinckmann, S., A. Engel, H. Bönisch, B. Quack, and E. Atlas, 2012: Short-lived brominated hydrocarbons – observations in the source regions and the tropical tropopause layer. *Atmos. Chem. Phys.*, **12**, 1213-1228, doi:10.5194/acp-12-1213-2012.

Carpenter, L. J., C. E. Jones, R. M. Dunk, K. E. Hornsby, and J. Woeltjen, 2009: Air-sea fluxes of

476 biogenic bromine from the tropical and North Atlantic Ocean. *Atmos. Chem. Phys.*, **9**, 1805–
477 1816, doi:10.5194/acp-9-1805-2009.
478 Carpenter, L. J., S. Reimann, (Lead Authors), J. B. Burkholder, C. Clerbaux, B. D. Hall, R.
479 Hossaini, J. C. Laube, and S. A. Yvon-Lewis, 2014: Ozone-Depleting Substances (ODSs) and
480 Other Gases of Interest to the Montreal Protocol. Chapter 1 in Scientific Assessment of Ozone
481 Depletion: 2014, Update on Global Ozone Research and Monitoring Project – Report No. 55,
482 World Meteorological Organization, Geneva, Switzerland.
483 Cotton, R., Osborne, S., Ulanowski, Z., Hirst, E., Kaye, P. H., and Greenaway, R., 2010: The ability
484 of the Small Ice Detector, SID2 to characterise cloud particle and aerosol morphologies obtained
485 during flights of the FAAM BAe-146 research aircraft. *J. Atmos. Ocean. Tech.*, **27**, 290–303.
486 Crosson, E.R., 2008: A cavity ring-down analyzer for measuring atmospheric levels of methane,
487 carbon dioxide, and water vapor. *Appl. Phys. B,* **92**, 403–408, doi:10.1007/s00340-008-3135-y.
488 Flemming, J., and Coauthors, 2015: Tropospheric chemistry in the Integrated Forecasting System of
489 ECMWF. *Geosci. Model Dev.*, **8**, 975-1003, doi:10.5194/gmd-8-975-2015.
490 Fueglistaler, S., A. E. Dessler, T. J. Dunkerton, I. Folkins, Q. Fu, and P. W. Mote, 2009: Tropical
491 tropopause layer. *Rev. Geophys.*, **47**, RG1004, doi:10.1029/2008RG000267.
492 Gerbig, C., S. Schmitgen, D. Kley, A. Volz-Thomas, K. Dewey, and D. Haaks, 1999: An improved
493 fast-response VUV resonance flourescence CO instrument. *J. Geophys. Res.*, **104**, 1699–1704.
494 Gettelman, A., M. L. Salby, and F. Sassi, 2002: Distribution and influence of convection in the
495 tropical tropopause region. J. *Geophys. Res.*, **107**, doi:10.1029/2001JD001048.
496 Gettelman, A., and Coauthors, 2009: The Tropical Tropopause Layer 1960–2100. *Atmos. Chem.*
497 *Phys.*, **9**, 1621-1637, doi:10.5194/acp-9-1621-2009.
498 Gostlow B., A. D. Robinson, N. R. P. Harris, L. O'Brien, D. E. Oram, G. P. Mills, H. M. Newton,
499 S. E. Yong and J. A. Pyle, 2010: Micro-DIRAC: An Autonomous Instrument for Halocarbon
500 Measurements. *Atmos. Meas. Tech.*, **3**, 507-521, doi:10.5194/amt-3-507-2010.
501 Heyes, W. J., G. Vaughan, G. Allen, G., A. Volz-Thomas, H.-W. Pätz, and R. Busen, R., 2009:
502 Composition of the TTL over Darwin: local mixing or long-range transport? *Atmos. Chem.*
503 *Phys.*, **9**, 7725-7736, doi:10.5194/acp-9-7725-2009.
504 Hirst, E., P. H. Kaye, R. S. Greenaway, P. Field, and D. W. Johnson, 2001: Discrimination of
505 micrometre-sized ice and super-cooled droplets in mixed-phase cloud. *Atmos. Environ.*, **35**, 33–
506 47, doi:10.1016/S1352-2310(00)00377-0.
507 Hopkins, J. R., K. A. Read, and A. C. Lewis, 2003*:* A Two Column Method For Long-term
508 Monitoring Of Non-Methane Hydrocarbons (NMHCs) and Oxygenated Volatile Organic
509 Compounds. *J. Environ. Mon*, **5**, 8-13.

510 Humpage, N., and Coauthors, 2014: GreenHouse Observations of the Stratosphere and Troposphere
511 (GHOST): a novel shortwave infrared spectrometer developed for the Global Hawk unmanned
512 aerial vehicle. *Proc. SPIE 9242, Remote Sensing of Clouds and the Atmosphere XIX; and Optics*
513 *in Atmospheric Propagation and Adaptive Systems XVII*, 92420P,
514 http://dx.doi.org/10.1117/12.2067330
515 Ishijima, K and Coauthors, 2010: Stratospheric influence on the seasonal cycle of nitrous oxide in
516 the troposphere as deduced from aircraft observations and model simulations. *J. Geophys. Res.*,
517 **115**, D20308, doi:10.1029/2009JD013322.
518 Jensen, E. J., and Coauthors, 2015: The NASA Airborne Tropical TRopopause EXperiment
519 (ATTREX): High-Altitude Aircraft Measurements in the Tropical Western Pacific. *Bull. Amer.*
520 *Meteor. Soc.*, submitted.
521 Kennedy, O. J., and Coauthors, 2011: An aircraft based three channel broadband cavity enhanced
522 absorption spectrometer for simultaneous measurements of NO_3, N_2O_5 and NO_2. *Atmos. Meas.*
523 *Tech.*, **4**, 1759-1776, doi:10.5194/amt-4-1759-2011.
524 Kaye, P.H., E. Hirst, R. S. Greenaway, Z. Ulanowski, E. Hesse, P. J. DeMott, C. Saunders, and P.
525 Connolly, 2008: Classifying atmospheric ice crystals by spatial light scattering. Opt. Lett., 33,
526 1545, doi:10.1364/OL.33.001545.
527 Lance, S., Brock, C. A., Rogers, D., and Gordon, J. A., 2010: Water droplet calibration of the Cloud
528 Droplet Probe (CDP) and in-flight performance in liquid, ice and mixed-phase clouds during
529 ARCPAC. *Atmos. Meas. Tech.*, 3, 1683-1706, doi:10.5194/amt-3-1683-2010.
530 Le Breton, M., and Coauthors, 2012: Airborne observations of formic acid using a chemical
531 ionization mass spectrometer, *Atmos. Meas. Tech.*, **5**, 3029-3039, doi:10.5194/amt-5-3029-2012.
532 Le Breton, M., and Coauthors, 2013: Airborne hydrogen cyanide measurements using a chemical
533 ionisation mass spectrometer for the plume identification of biomass burning forest fires, *Atmos.*
534 *Chem. Phys.*, **13**, 9217-9232, doi:10.5194/acp-13-9217-2013.
535 Lee, J. D., S. J. Moller, K. A. Read, A. C. Lewis, L. Mendes, and L. J. Carpenter, 2009: Year-round
536 measurements of nitrogen oxides and ozone in the tropical North Atlantic marine boundary
537 layer. *J. Geophys.Res.*, **114**, D21302, DOI:10.1029/2009JD011878
538 Lenschow, D. H., 1986: Probing the atmospheric boundary layer. Chap. in *Aircraft measurements*
539 *in the boundary layer*, 39–55, Amer. Meteor. Soc..
540 Levine, J. G., P. Braesicke, N. R. P. Harris, N. H. Savage, and J. A. Pyle, 2007: Pathways and
541 timescales for troposphere-to-stratosphere transport via the tropical tropopause layer and their
542 relevance for very short lived substances. *J. Geophys. Res.*, **112**, D04308,
543 doi:10.1029/2005JD006940.

544 Levine, J. G., P. Braesicke, N. R. P. Harris, and J. A. Pyle, 2008: Seasonal and inter-annual
545 variations in troposphere-to-stratosphere transport from the tropical tropopause layer. *Atmos.*
546 *Chem. Phys.*, **8**, 3689-3703, doi:10.5194/acp-8-3689-2008.
547 Lewis, A.C., and Coauthors, 2013: The Influence of Forest Fires on the Global Distribution of
548 Selected Non-Methane Organic Compounds. *Atmos. Chem. Phys.*, **13**, 851-867, doi:10.5194/acp-
549 13-851-2013.
550 Liu, D., and Coauthors, 2015: The importance of Asia as a source of black carbon to the European
551 Arctic during springtime 2013. *Atmos. Chem. Phys.*, **15**, 11537-11555, doi:10.5194/acp-15-
552 11537-2015.
553 Long, C. N., and Coauthors, 2013: ARM Research In The Equatorial Western Pacific: A Decade
554 And Counting. *Bull. Amer. Meteor. Soc.*, **94**, 695–708. doi:10.1175/BAMS-D-11-00137.1.
555 Mather, J. H., T. P. Ackerman, W. E. Clements, F. J. Barnes, M. D. Ivey, L. D. Hatfield, and R. M.
556 Reynolds, 1998: An Atmospheric Radiation and Cloud Station in the Tropical Western Pacific.
557 *Bull. Amer. Meteor. Soc.*, **79**, 627–642. doi:10.1175/1520-0477.
558 Navarro, M. A., and Coauthors, 2015: Airborne measurements of organic bromine compounds in
559 the Pacific tropical tropopause layer. *Proc. Nat. Acad. Sci.*, doi:10.1073/pnas.1511463112.
560 Newton, R., G. Vaughan, H. M. A. Ricketts, L. L. Pan, A. J. Weinheimer, and C. Chemel, 2015:
561 Ozonesonde profiles from the West Pacific Warm Pool, *Atmos. Chem. Phys. Discuss.*, **15**,
562 16655-16696, doi:10.5194/acpd-15-16655-2015.
563 O'Shea, S. J., S. J.-B. Bauguitte, M. W. Gallagher, D. Lowry, and C. J. Percival, 2013:
564 Development of a cavity-enhanced absorption spectrometer for airborne measurements of CH_4
565 and CO_2. *Atmos. Meas. Tech.*, **6**, 1095-1109, doi:10.5194/amt-6-1095-2013.
566 Pan, L. L., and Co-authors, 2015a: Bimodal distribution of free tropospheric ozone over the tropical
567 western Pacific revealed by airborne observations. *Geophys. Res. Lett.*, **42**,
568 doi:10.1002/2015GL065562.
569 Pan, L. L., and Co-authors, 2015b: The Convective Transport of Active Species in the Tropics
570 (CONTRAST) Experiment. *Bull. Amer. Meteor. Soc.,* submitted.
571 Petersen, G. N., and I. A. Renfrew, 2009: Aircraft-based observations of air–sea fluxes over
572 Denmark Strait and the Irminger Sea during high wind speed conditions. *Q. J. R. Meteorol. Soc.,*
573 **135**, 2030–2045, 10.1002/qj.355.
574 Platnick, S., and Co-authors, 2015: MODIS Atmosphere L2 Cloud Product (06_L2). NASA
575 MODIS Adaptive Processing System, Goddard Space Flight Center, USA:
576 http://dx.doi.org/10.5067/MODIS/MYD06_L2.006
577 Randel, W., and E. Jensen, 2013: Physical processes in the tropical tropopause layer and their roles
578 in a changing climate. *Nature Geoscience*, **6**, 169-176, doi:10.1038/ngeo1733.

Robinson, A.D., and Co-authors, 2014: Long term halocarbon observations from a coastal and an inland site in Sabah, Malaysian Borneo. *Atmos. Chem. Phys.*, **14**, 8369-8388, doi:10.5194/acp-14-8369-2014.

Rosenberg, P.D., A. R. Dean, P. I. Williams, J. R. Dorsey, A. Minikin, M. A. Pickering, and A. Petzold, 2012: Particle sizing calibration with refractive index correction for light scattering optical particle counters and impacts upon PCASP and CDP data collected during the Fennec campaign. *Atmos. Meas. Tech.*, **5**, 5, 1147-1163, 10.5194/amt-5-1147-2012.

Ström, J., R. Busen, M. Quante, B. Guillemet, P. R. A. Brown, and J. Heintzenberg, 1994: Pre-EUCREX intercomparison of airborne humidity measuring instruments. *J. Atmos. Tech.*, **11**, 1392–1399, 1994.

Ulanowski, Z., Kaye, P. H., Hirst, E., Greenaway, R. S., Cotton, R. J., Hesse, E., and Collier, C. T., 2014: Incidence of rough and irregular atmospheric ice particles from Small Ice Detector 3 measurements. *Atmos. Chem. Phys.*, **14**, 1649-1662, doi:10.5194/acp-14-1649-2014.

Whalley, L. K., A. C. Lewis, J. B. McQuaid, R. M. Purvis, J. D. Lee, K. Stemmler, C. Zellweger, and P. Ridgeon, 2004: Two high-speed, portable GC systems designed for the measurement of nonmethane hydrocarbons and PAN: Results from the Jungfraujoch high altitude observatory. *J. Env. Mon.*, **6**, 234-241.

Wilson, K. L., and J. W. Birks, 2006: Mechanism and elimination of a water vapor interference in the measurement of ozone by UV absorbance. *Env. Sci. & Tech.,* **40**, 6361-6367, DOI: 10.1021/es052590c.

Wofsy, S.C., and Coauthors, 2011: HIAPER Pole-to-Pole Observations (HIPPO): fine-grained, global-scale measurements of climatically important atmospheric gases and aerosols. *Phil. Trans. R. Soc. A,* **369**, 2073–2086, doi: 10.1098/rsta.2010.0313.

603 Table 1: Instruments and measurements made on the BAe 146 (FAAM) aircraft during the CAST project. The table also indicates the synergy with
604 other aircraft from the CONTRAST (Gulfstream-V (GV)) and ATTREX (Global Hawk (GH) projects.

Species / parameter	**Method / instrument details**	**Averaging time**	**Precision, accuracy**	**Synergy with other aircraft**	**Affiliation, reference**
Position, winds, u, v, w	INS, GPS, 5-port turbulence probe	0.1 s	0.01 $\Delta P/P_S$	GV, GH	FAAM Peterson and Renfrew (2009)
Humidity (Dew point T)	Hygrometer, General Eastern 1011b	0.25 s	± 0.5 - ± 3 K dependent on dew point and ambient conditions	GV, GH	FAAM Ström et al. (1994)
Temperature	Rosemount Aerospace Ltd. sensor 102 AL	.05 s	± 0.3K	GV, GH	FAAM Lenschow (1986)
CO	VUV resonance / fluorescence, Aerolaser 5002	1 s	1 ppb, 3%	GV, GH	FAAM Gerbig et al. (1999)
O_3	UV absorption, TEI 49C	4 s	1 ppb, ±5%	GV, GH	FAAM Wilson and Birks (2006)
CO_2, CH_4	Cavity enhanced absorption spectrometer, Los Gatos Research Inc	1 s	CH_4: 2.5 ppb; 1.3 ppm CO_2: 0.7 ppm; 0.2 ppm	GV, GH	FAAM / U. Manchester O'Shea et al. (2013)
NO, NO_2	Chemiluminescence with photolytic conversion for NO_2, Air Quality Design Inc.	10 s	5 pptv for NO and 15 pptv for NO_2 (at 10 s averaging)	GV	FAAM / U. York Lee et al. (2009)
Halocarbons (Whole air samples (WAS)): (DMS, $CHBr_3$, CH_2Br_2, $CHBr_2Cl$, CH_3I, CH_2BrCl, $CHBrCl_2$, CH_2ICl, CH_2IBr, CH_2I_2, CH_2Cl_2, $CHCl_3$)	TD-GC-MS, Markes	30 s fill time for WAS	Species dependent, typically 0.1 – 1 pptv.	GV, GH	U. York Andrews et al. (2013; 2015)
NMHCs (Whole air samples (WAS)): (C^1-C^7 NMHCs (alkanes, alkenes, aromatics); small o-VOCs (acetone, methanol, acetaldehyde, ethanol); DMS	GC-FID (flame ionization detector), Perkin Elmer	30 s fill time for WAS	Species dependent, typically 5 pptv	GV, GH	U. York Hopkins et al. (2003)
Halocarbons, VOCs *(in situ)*	GC-MS (Gas Chromatography – Mass Spectrometry), Agilent	300 s	Species dependent, typically 1 – 5 pptv.	GV	U. York
BrO, Br_2, HOBr, BrCl, HCOOH (formic acid), HCN, $ClNO_2$, HNO_3, N_2O_5, CH_3COOH (acetic acid), CH_3CH_2COOH (propanoic acid), $CH_3CH_2CH_2COOH$ (butanoic acid)	Chemical Ionisation Mass Spectrometer (CIMS)	30 s	Species dependent, typically 0.3 – 5 ppt	GV	U. Manchester Le Breton et al. (2012)
IO	Broadband Cavity Enhanced	*see text*	*see text*	GV (IO	U. Cambridge

Aerosol	PCASP (Passive Cavity Aerosol Spectrometer Probe)	1s	See text	GV, GH	FAAM Rosenberg et al., (2012)
Cloud physics	CDP (Cloud Droplet Probe)	1s	See text	GV, GH	FAAM Rosenberg et al., (2012)

Table 2: Measurements made at the ARM site at Manus, Papua New Guinea during CAST

Species / parameter	**Method / instrument details**	**Operation**	**Precision, accuracy**	**Affiliation, reference**
O_3 (profile)	Ozonesonde, ENSCI model Z from DMT	Daily	see Newton et al 2015	U. Manchester, NCAS Newton et al 2015
O_3 (surface)	Thermo-49 analyser	Continuous (10 sec)	± 1 ppbv, precision-limited	NCAS, Atmospheric Measurement Facility
CO_2, CH_4	Picarro G2401 CRDS analyser	Continuous (5 sec)	CO_2 precision 0.05 %, accuracy 0.05 % (±1sd); CH_4 precision 0.05 %, accuracy 0.1 % (±1sd);	U. Cambridge Crosson (2008)
Halocarbons: ($CHBr_3$, $CHBr_2Cl$, CH_3I, CH_2ICl, C_2Cl_4)	Custom-built GC-ECD	Continuous (~50 minutes)	Species dependent, typically 0.1 – 1 pptv.	U. Cambridge Gostlow et al, (2010), Robinson et al., (2014)

Information about the meteorological measurements from Manus can be found at http://www.arm.gov/sites/twp/C1/instruments.

612 Table 3: Research flights made by the BAe 146 (FAAM) aircraft during the CAST project.

Flight no.	Date	Route	Flight description and observations
B823	18/1/14	Kota Kinabalu - Palau - Guam	Measurements on last part of leg from KK to Palau. Flight mainly at low levels (in boundary layer) on Palau to Guam leg. O_3 and CO decreasing further North (O_3 30-12 ppb), higher (>35ppb) above boundary layer (BL).
B824	22/1/14	Guam – Guam	Heading SE from Guam, 4000 m then 2000 m, flight aborted early due to aircraft technical problem. GV followed around 30 minutes later. O_3 15 ppb near Guam, falling to 10 ppb at 7°S.
B825	24/1/14	Guam – Chuuk	Mixed altitudes (lowest 300 m), mainly within BL. O_3 dropping from 15 ppb to 8 ppb towards Chuuk. CO ~105 ppb on whole flight. SE flow.
B826	25/1/14	Chuuk – Chuuk	Due South from Chuuk on 152°E to 2°N, back on 153°E. Start at 6000 m then step down to 300 m. O_3 constant (~15 ppb) in boundary layer, 25 ppb above BL. Largely SE flow in BL, W-NW in free troposphere.
B827	26/1/14	Chuuk – Chuuk	Due South from Chuuk on 152°N to 1°N then return on same track. In BL to 1°N, 4000 m on return North. Well mixed boundary layer. 20 ppb O_3 to 1°N. BrO and CH_2Cl_2 observed. Largely SE flow in BL, W-NW in FT.
B828	26/1/14	Chuuk - Guam	Circled atoll at 100 m and 1500 m; then mixed altitude down to 300 m on way back to Guam. CO 100ppb round atoll in BL, O_3 15 ppb. O_3 10-13ppb as head North towards Guam.
B829	29/1/14	Guam - Palau	Mixed levels in BL down to 300 m. Low O_3 (12 ppb) observed around island of Yap. Easterly flow.
B830	29/1/14	Palau – Palau	Flight East along 7°N; mixed altitude down to 300 m; 4 stacked runs above each other at easterly end. Profile of BrO observed on stacked runs - higher at surface. Same CO and O_3 profile at all levels so well mixed BL. 45 ppb O_3 and some NOx (25 ppt) seen at 4000 m. Higher N_2O at higher altitudes. Largely SE flow.
B831	30/1/14	Palau – Palau	Flight SE to Indonesian airspace (4°30'N, 141°30'E) then due South to 3°N. Mainly in BL, down to 300 m at most Southern point where O_3 was 25-30 ppb. Westerly flow so some Asian outflow observed (CO < 100 ppb).
B832	30/1/14	Palau – Guam	Low level runs in BL crossing day/night terminator. 30m in early part of flight before hitting low level convection. Above BL towards Guam. 15 ppb O_3 during sunset - very constant as heading North. NW flow.
B833	1/2/14	Guam – Guam	1st part of day/night chemistry flights. Stacked legs to E of Guam: 6000, 3000, 1500, 1000, and 300 m. NE flow. Followed GV for first half of flight (~30 minutes behind).
B834	1/2/14	Guam – Guam	2nd part of day/night chemistry flights. Stacked legs to E of Guam: 6000, 3000, 1500, 1000, and 300 m. NE flow.
B835	4/2/14	Guam – Chuuk	Fast transit to Chuuk above BL. 25 ppb O_3, 85 ppb CO at 6000 m, then O_3 lower as dropping down to Chuuk (~13 ppb).

B836	4/2/14	Chuuk – Chuuk	Head S along 152°E at 7000 m, some low flying in BL to southern most point (1°S) before intermediate height (2000 – 4000 m) back to Chuuk. 18 ppb O_3 above BL to 1°N. Then profile down and less O_3 in BL (13 ppb), CO 70 ppb. At 1°S O_3 9 ppb in NE flow.
B837	5/2/14	Chuuk – Chuuk	Low level flying in BL to southernmost point (~1°N) to complement B836), then climb back and return at ~5000 m. O_3 decreasing in BL as head South. 20 ppb at 7°N, 11 ppb at 1°N. All in NE flow.
B838	6/2/14	Chuuk – Chuuk	Round Chuuk atoll at 3 altitudes in BL (150, 500, and 1000 m). CO higher to East of Islands (Easterly flow). Could be storms over the islands bringing elevated CO to the upwind side.
B839	12/2/14	Chuuk – Guam	SE of Guam at low level (500 m in BL), then above BL (5000 m) before descending down at lower levels in BL into Guam. O_3 spikes in profiles up to 7500 m (Asian outflow). 75 ppb seen at 7000 m.
B840	13/2/14	Guam – Palau	Start in FT (~6500 m), then low nearer Palau (1500 m); head to 4°N, 137°E before heading NW; same region as GV and GH. O_3 30 ppb in FT, 12 ppb in BL, very stable. Easterly flow.
B841	14/2/14	Palau – Palau	Flight to SW of Palau with stacked legs in BL parallel to ATC boundary. O_3 15 ppb in BL. Easterly flow.
B842	14/2/14	Palau - Guam	Reverse flight to B840. Similar flow and O_3.
B843	16/2/14	Guam – Guam	S from Guam to 7°N then E towards Chuuk before heading back to Guam; low latitude parts at low altitudes (<1000 m in BL) under convective band. O_3 10-15 ppb in BL (E flow), elevated at higher levels (70-90 ppb), concurrent with elevated NO (30 ppt) (N flow).
B844	17/2/14	Guam – Guam	SSE from Guam to fly under convective band (to 4°N) with low level runs (< 1000 m in BL). GV and GH flying nearby. Layers of elevated O_3 and NO_x at ~6000m (westerly flow).
B845	17/2/14	Guam – Guam	S from Guam to be West of convective band (to 6°N). Low level legs (< 1000 m in BL) at Southern end. Layers of elevated O_3 and NO_x at ~6000 m (westerly flow).
B846	18/2/14	Guam - Palau	Start in FT (~6500 m), then low nearer Palau (1500 m); head to 4°N, 137°E before heading NW; same region as GV and GH. O_3 30 ppb in FT, 12 ppb in BL, very stable. Easterly flow.
B847	18/2/14	Palau – Kota Kinabalu	Steady ascent toward KK. Some Asian outflow observed on initial ascent (CO ~ 140 ppb). Westerly flow.

613

Figure Caption List

Figure 1: Map of FAAM BAe-146 flight tracks during January and February 2014. The flights tracks are coloured by altitude. The islands of Guam, Palau and Chuuk are marked. The background shows Jan-Feb averaged Chlorophyll-a concentrations, measured by the MODIS satellite (NASA Giovanni, Acker et al., 2007). The inset shows an enlarged area around Chuuk Atoll.

Figure 2: Ozone and carbon monoxide mixing ratios measured in all CAST flights as a function of latitude and altitude. See text and Table 1 for instrumental details.

Figure 3: Plots of O_3 against CO coloured by (upper) NO and (lower) relative humidity (10 s averaged data).

Figure 4: $CHBr_3$ mixing ratios (colours) sampled on the FAAM aircraft during CAST using the whole air sampler (squares) and the on-board GC-MS (circles). Panel (a) contains all measurements made at altitudes less than 1 km, and the enlarged inset (bottom left) shows the values around the Chuuk Atoll. The lines associated with each measurement indicate the instantaneous wind speed measured by the aircraft. Panel (b) contains the measurements at altitudes greater than 1 km, and the inset shows the vertical profile of all measurements.

Figure 5: Surface observations of wind, O_3, CO_2, CH_4, C_2Cl_4, $CHBr_3$ and CH_3I at the ARM Facility on Manus Island, Papua New Guinea (2.07°S, 147.4°E) from February 1-24, 2014. The time shown in the x-axis is Universal Time. The shading indicates the local time, with the darker bands representing night-time.

Figure 6: Daily observed ozone profile in Manus (left) and corresponding MACC forecast with a lead time of 1 day (middle) and 4 days (right).

Figure 7. Examples of trajectory-based forecast products used for multi-aircraft flight planning. These plots are for February 13 2014 when all three aircraft were in the same region (see Figure 7 in Pan et al. (2015b)). The three panels show the location of air parcels which had been below 1 km altitude in the preceding 12 days at (a) 16-18 km; (b) 14-16 km; and (c) 12-14 km. The number in each box is the percentage of parcels in that box from below 1 km in the preceding 12 days. During the campaign, they were available as

649 1, 3 and 5 day forecasts for flight planning, and the NAME model was driven by
650 analyses and forecasts from Met Office operational model run at 25 km horizontal
651 resolution.
652
653 Figure 8: AIITS scattering patterns recorded from ice particles in the UTLS, at altitudes of ~ 16
654 km and temperatures of ~ -80°C. The pictures are indicative of (left) a smooth quasi-
655 spherical ice particle, (middle) a columnar crystal, and (right) a pristine hexagonal plate.
656
657 Figure 9: Flight path of the NASA Global Hawk on 10th March 2015 (blue). OCO-2 (green) and
658 GOSAT (red) soundings are shown which coincide temporally with the flight leg
659 between 25°N, 127°W and 18°N, 125°W. MODIS cloud fraction data (Platnick et al.,
660 2015) coincident with the OCO-2 overpass at 2140 UTC is plotted in grayscale,
661 showing the largely cloud-free conditions encountered during this leg of the flight.
662
663

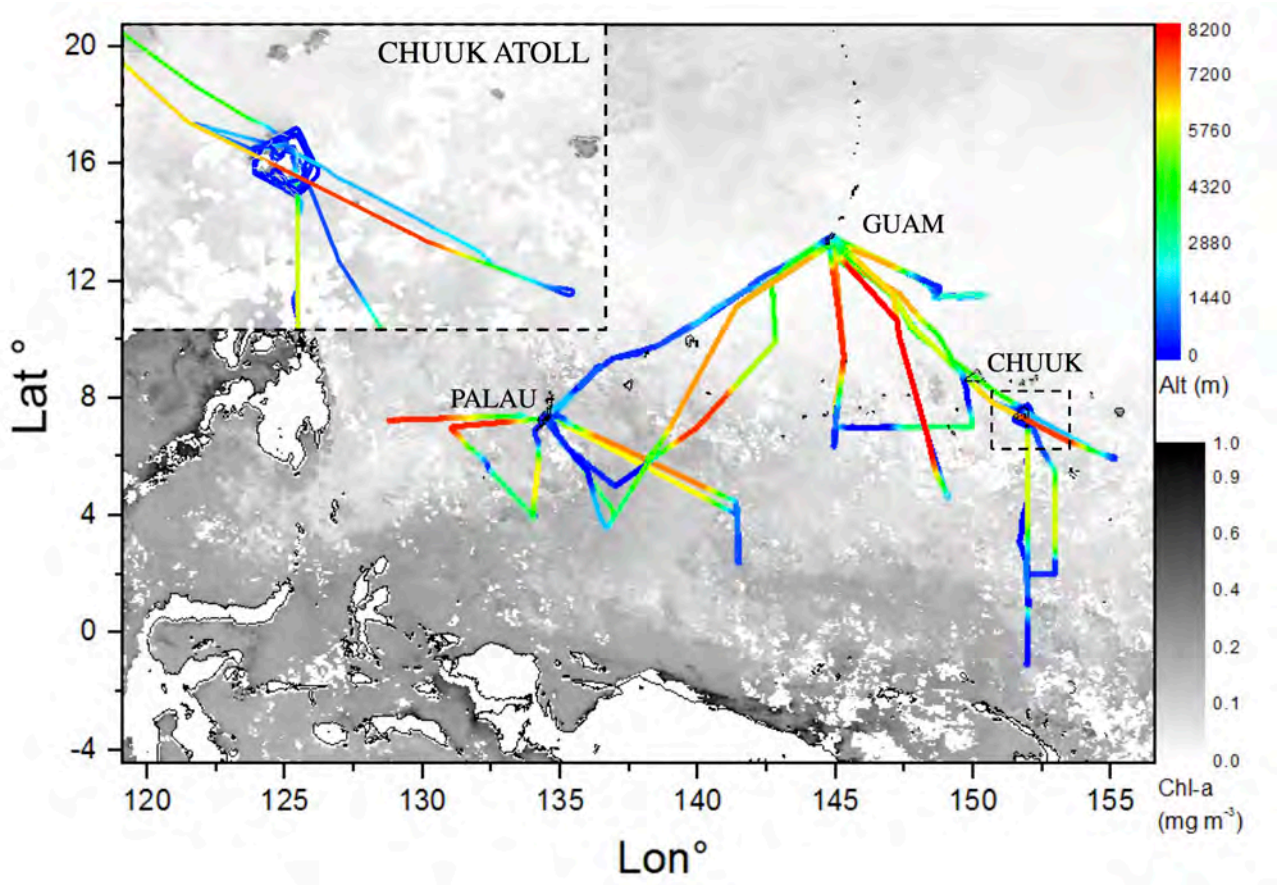

Figure 1: Map of FAAM BAe-146 flight tracks during January and February 2014. The flights tracks are coloured by altitude. The islands of Guam, Palau and Chuuk are marked. The background shows Jan-Feb averaged Chlorophyll-a concentrations, measured by the MODIS satellite (NASA Giovanni, Acker et al., 2007). The inset shows an enlarged area around Chuuk Atoll.

673

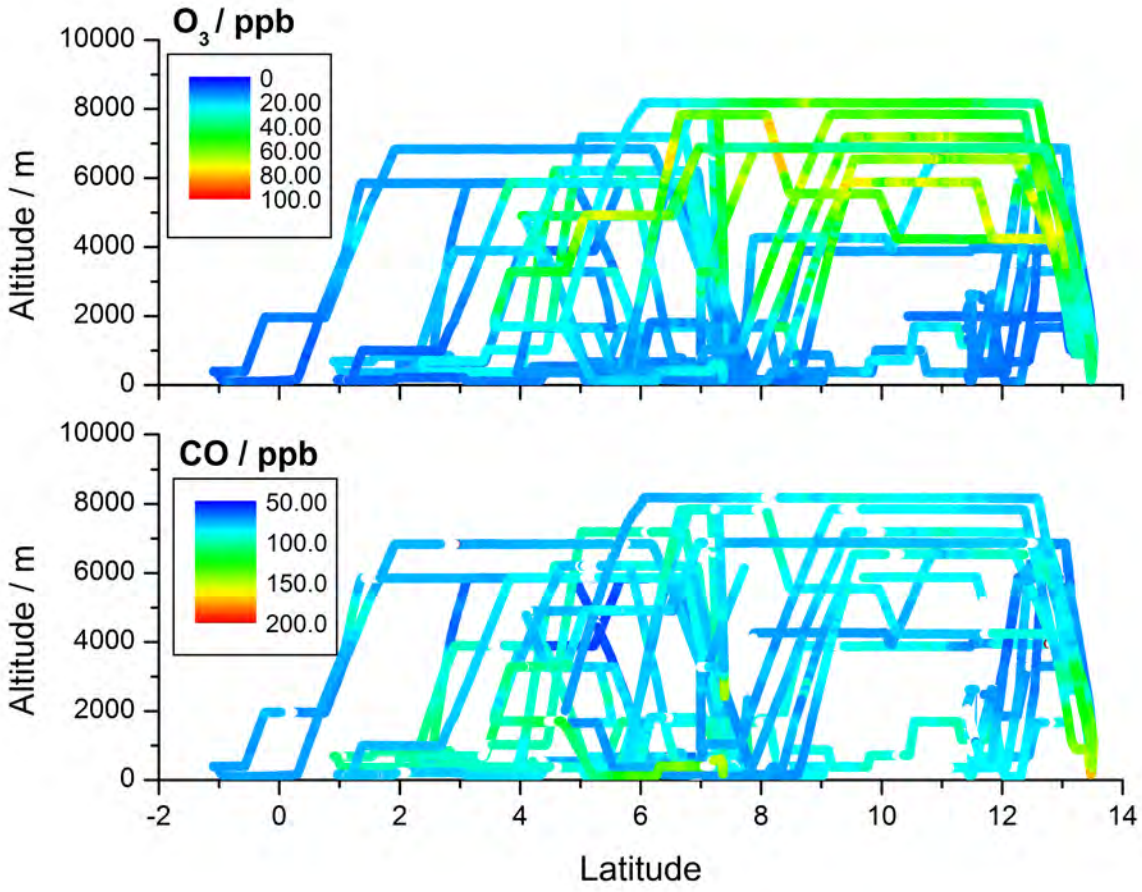

674

675

676 Figure 2: Ozone and carbon monoxide mixing ratios measured in all CAST flights as a function
677 of latitude and altitude. See text and Table 1 for instrumental details.

678

679

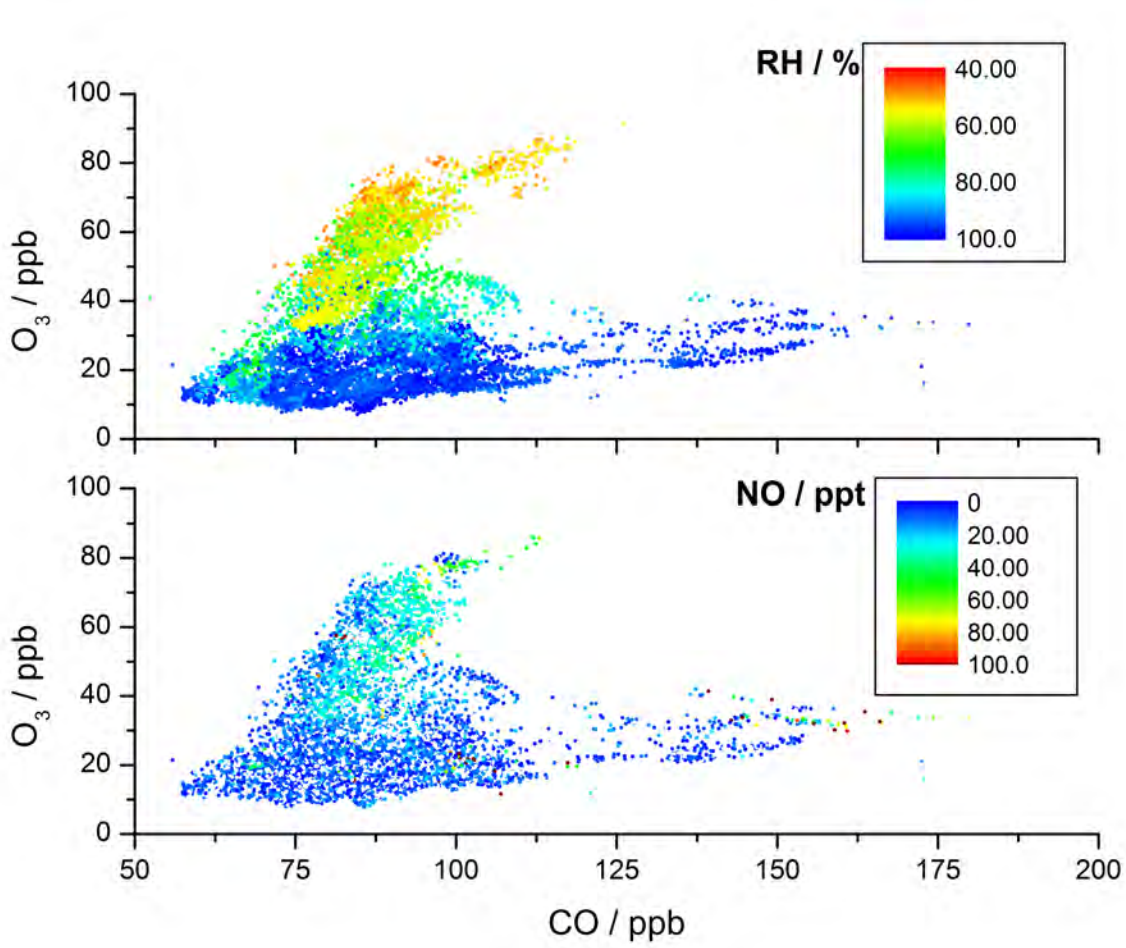

680

681

682

683 Figure 3: Plots of O_3 against CO coloured by (upper) NO and (lower) relative humidity (10 s

684 averaged data).

685

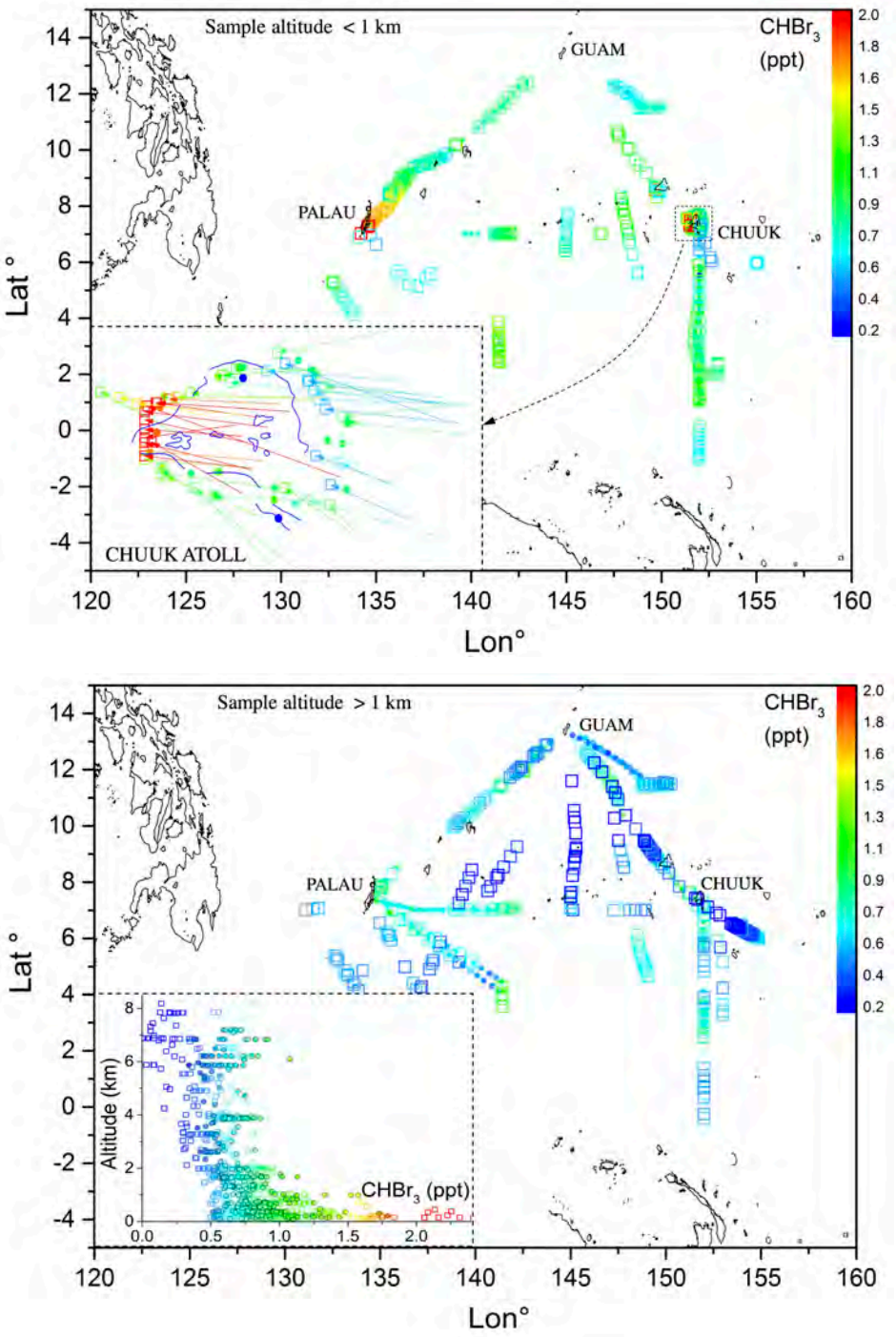

Figure 4: $CHBr_3$ mixing ratios (colours) sampled on the FAAM aircraft during CAST using the whole air sampler (squares) and the on-board GC-MS (circles). Panel (a) contains all measurements made at altitudes less than 1 km, and the enlarged inset (bottom left) shows the values around the Chuuk Atoll. The lines associated with each measurement indicate the instantaneous wind speed measured by the aircraft. Panel (b) contains the measurements at altitudes greater than 1 km, and the inset shows the vertical profile of all measurements.

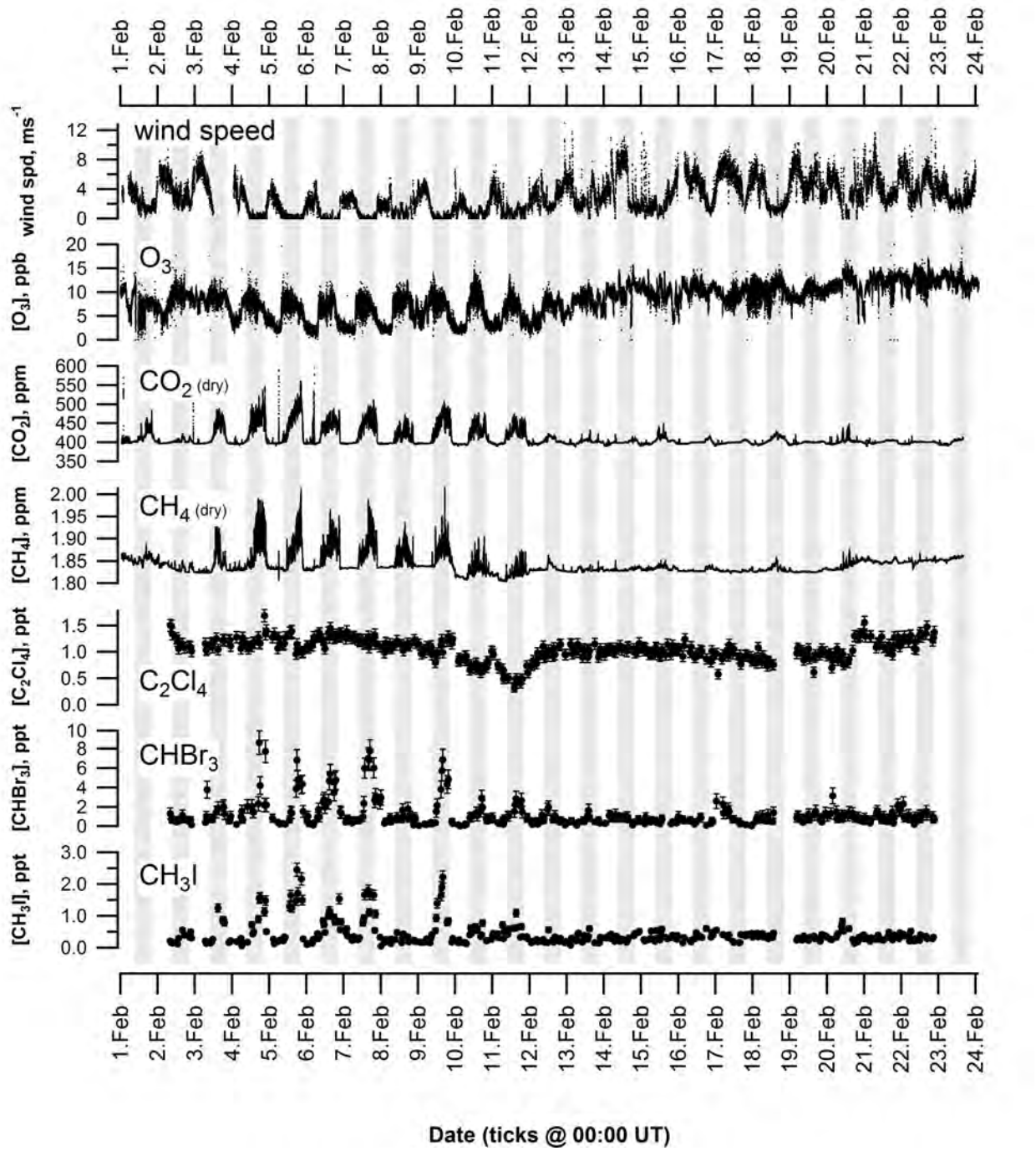

Figure 5: Surface observations of wind, O_3, CO_2, CH_4, C_2Cl_4, $CHBr_3$ and CH_3I at the ARM Facility on Manus Island, Papua New Guinea (2.07°S, 147.4°E) from February 1-24, 2014. The time shown in the x-axis is Universal Time. The shading indicates the local time, with the darker bands representing night-time.

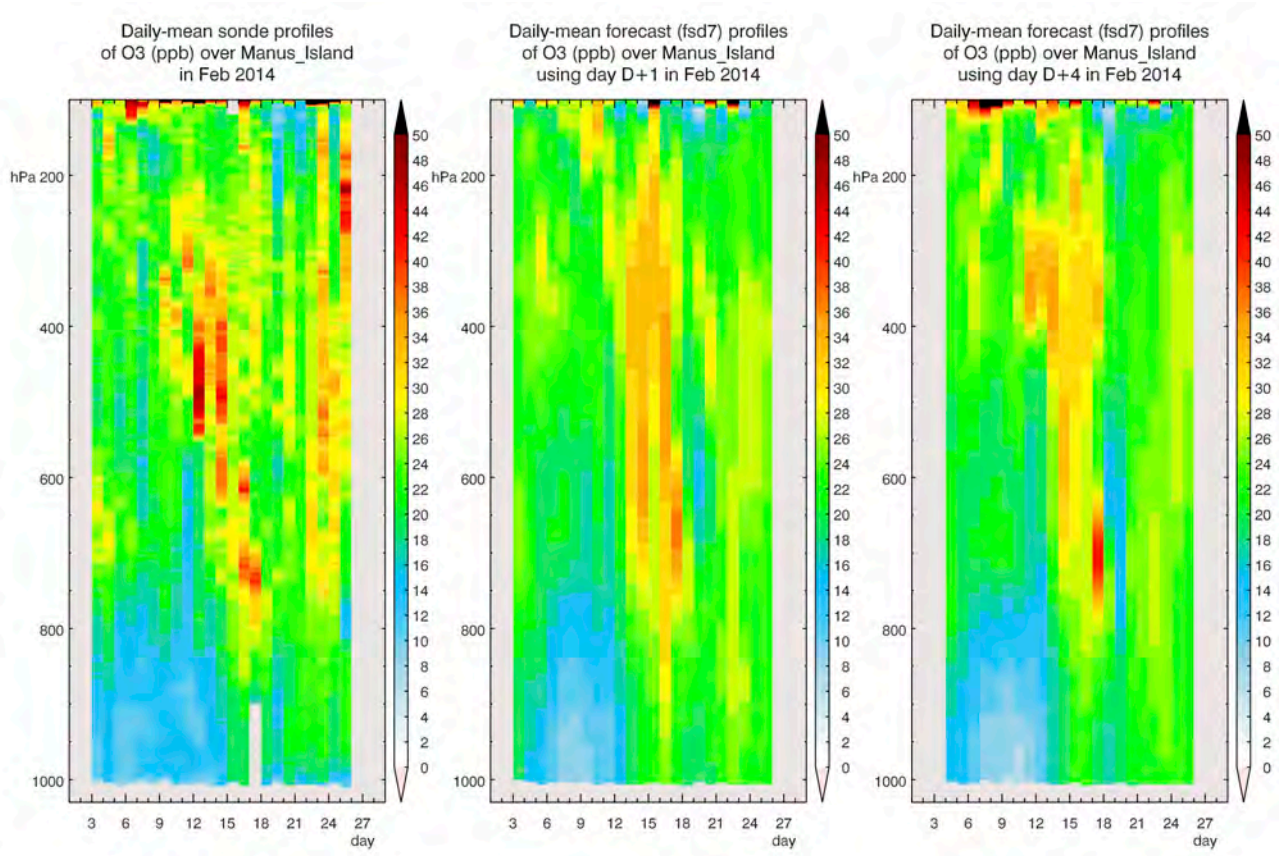

Figure 6: Daily observed ozone profile in Manus (left) and corresponding MACC forecast with a lead time of 1 day (middle) and 4 days (right).

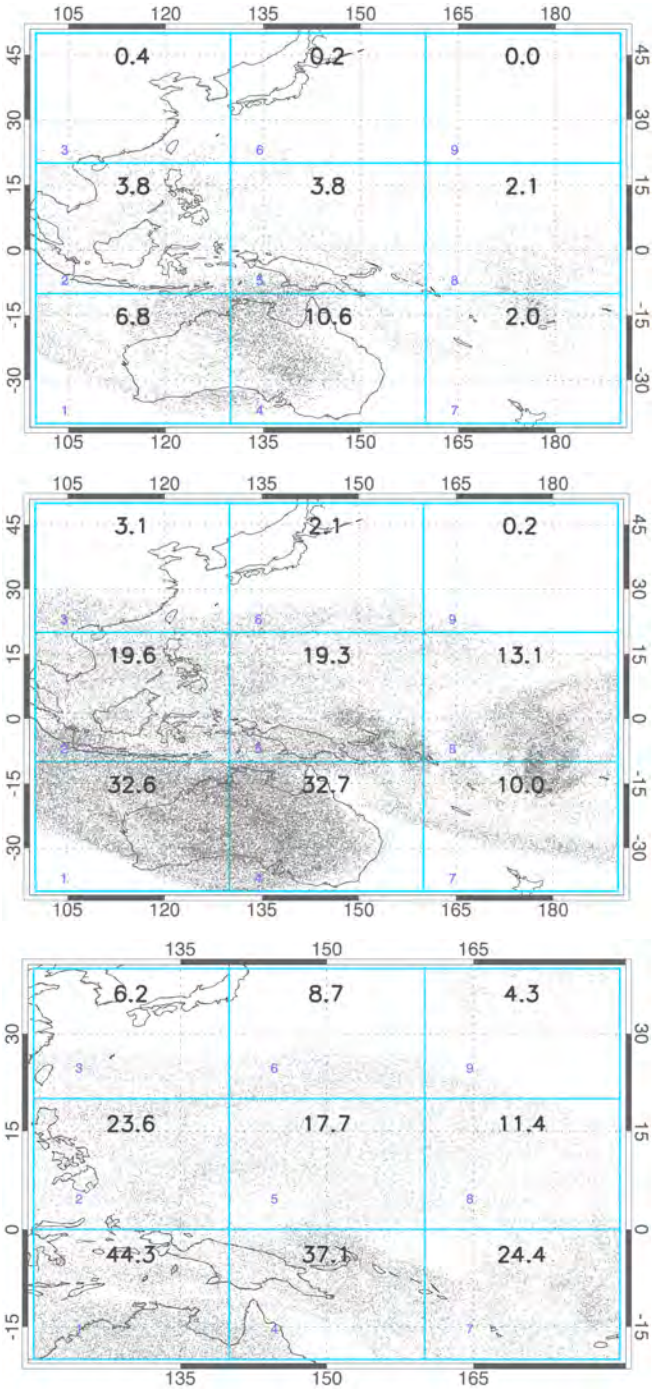

711

712

713

714 Figure 7. Examples of trajectory-based forecast products used for multi-aircraft flight
715 planning. These plots are for February 13 2014 when all three aircraft were in the
716 same region (see Figure 7 in Pan et al. (2015b)). The three panels show the location
717 of air parcels which had been below 1 km altitude in the preceding 12 days at (a) 16-
718 18 km; (b) 14-16 km; and (c) 12-14 km. The number in each box is the percentage
719 of parcels in that box from below 1 km in the preceding 12 days. During the
720 campaign, they were available as 1, 3 and 5 day forecasts for flight planning, and the
721 NAME model was driven by analyses and forecasts from Met Office operational
722 model run at 25 km horizontal resolution. *NB Only a fraction of the trajectories are*
723 *shown in each plot, so the density of dots is not comparable at different altitudes.*

724

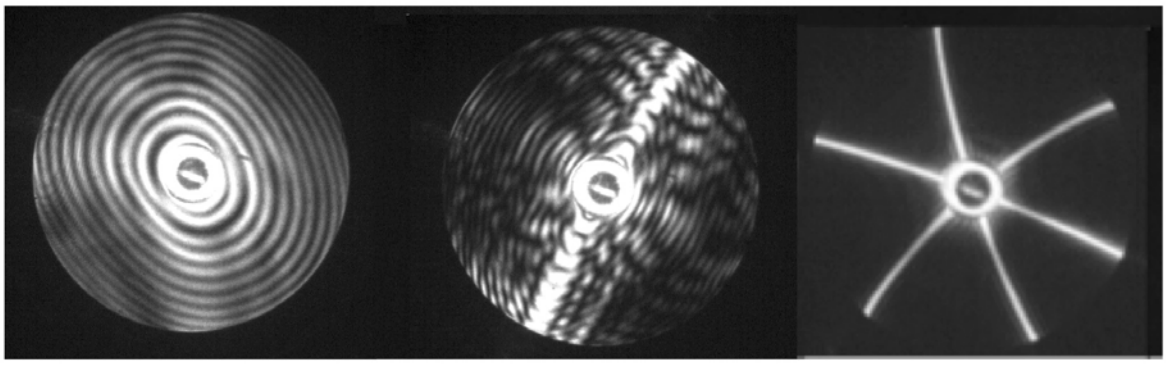

725
726
727
728 Figure 8: AIITS scattering patterns recorded from ice particles in the UTLS, at altitudes of ~ 16
729 km and temperatures of ~ -80^{o}C. The pictures are indicative of (left) a smooth quasi-
730 spherical ice particle, (middle) a columnar crystal, and (right) a pristine hexagonal plate.
731
732

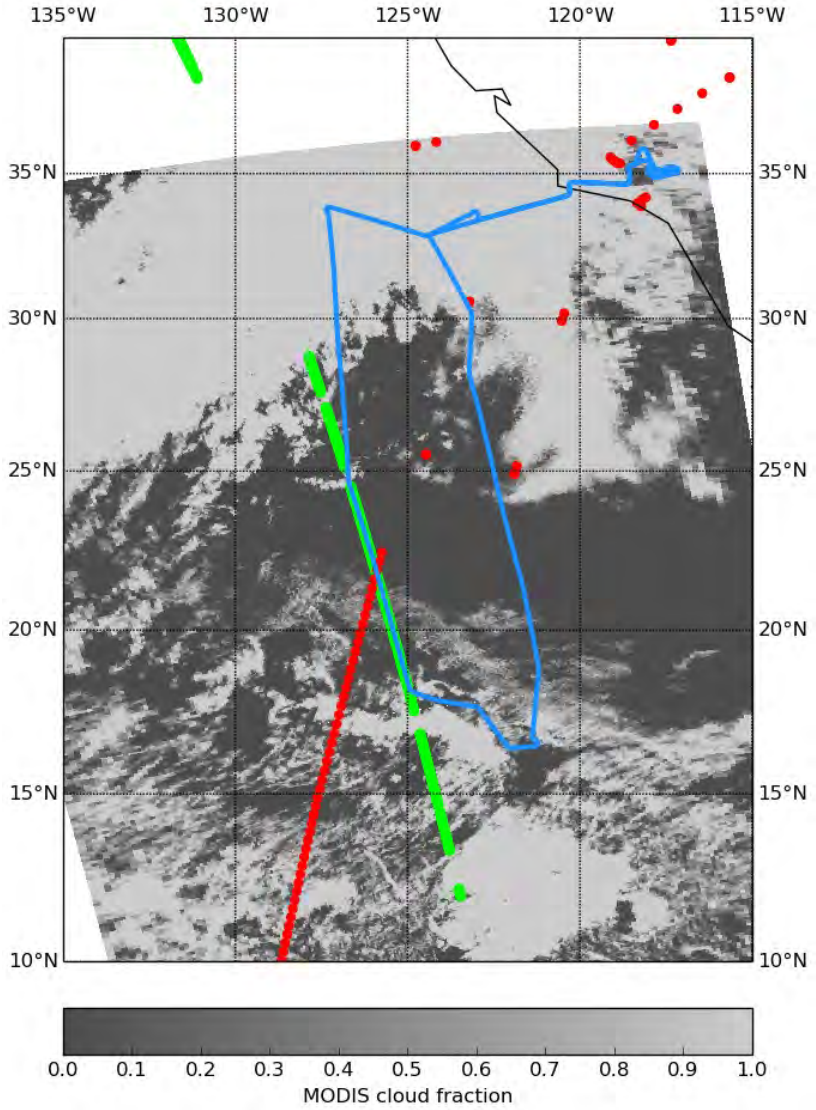

Figure 9: Flight path of the NASA Global Hawk on 10th March 2015 (blue). OCO-2 (green) and GOSAT (red) soundings are shown which coincide temporally with the flight leg between 25°N, 127°W and 18°N, 125°W. MODIS cloud fraction data (Platnick et al., 2015) coincident with the OCO-2 overpass at 2140 UTC is plotted in grayscale, showing the largely cloud-free conditions encountered during this leg of the flight.